Appl. Phys. A (2017) 123:230
DOI 10.1007/s00339-017-0802-z

Applied Physics A
Materials Science & Processing

Surface laser marking optimization using an experimental design approach

F. Brihmat-Hamadi[1] · E. H. Amara[1] · L. Lavisse[2] · J. M. Jouvard[2] · E. Cicala[3] · H. Kellou[4]

Received: 12 April 2016 / Accepted: 20 January 2017

Abstract Laser surface marking is performed on a titanium substrate using a pulsed frequency doubled Nd:YAG laser (λ= 532 nm, τ_{pulse}=5 ns) to process the substrate surface under normal atmospheric conditions. The aim of the work is to investigate, following experimental and statistical approaches, the correlation between the process parameters and the response variables (output), using a Design of Experiment method (DOE): Taguchi methodology and a response surface methodology (RSM). A design is first created using MINTAB program, and then the laser marking process is performed according to the planned design. The response variables; surface roughness and surface reflectance were measured for each sample, and incorporated into the design matrix. The results are then analyzed and the RSM model is developed and verified for predicting the process output for the given set of process parameters values. The analysis shows that the laser beam scanning speed is the most influential operating factor followed by the laser pumping intensity during marking, while the other factors show complex influences on the objective functions.

✉ E. H. Amara
amara@cdta.dz

[1] Centre de Développement des Technologies Avancées, Laser Material Processing Team, PO. Box 17 Baba-Hassen, 16303 Algiers, Algeria

[2] Laboratoire Interdisciplinaire Carnot de Bourgogne, UMR 5209 CNRS-Université de Bourgogne, 1 allée des Granges Forestier, 71100 Chalon sur Saône, France

[3] Laboratoire Interdisciplinaire Carnot de Bourgogne, UMR 5209 CNRS-Université de Bourgogne, 12 Rue de la Fonderie, 71200 Le Creusot Cedex, France

[4] Quantum Electronics Laboratory, Faculty of Physics, Université des Sciences et de la Technologie Houari Boumedienne, PO. Box 32 El-Alia, Bab-Ezzouar, Algiers, Algeria

1 Introduction

Metals surface coloration induced during laser treatment offers many interesting applications in miscellaneous fields such as manufactured products identification [1], fight against counterfeiting [2], aesthetics and arts [3–5], etc. Its main advantage in comparison with the conventional marking processes is the no using and no generation of toxic products in regards to the environmental protection. Its principle is based on the interaction of laser beam pulses with the material surface, under normal or controlled atmospheric pressure conditions. Under the normal atmospheric conditions, the colors generation results from surface oxidation during the laser beam heating of the material surface. The obtained colors are related to the the laser beam operating parameters such as its power, its pulses frequency, its scanning velocity, its spot diameter, as well as to the substrate physical properties, including its thickness, and to the environmental conditions.

The obtained surface treatment is a thermal process modifying the superficial properties, without significant changes of the basic material properties. Earlier work [7–10] showed that when a pulsed laser (Nd:YAG) interacts with a titanium surface, under normal atmospheric pressure, it forms one or more layers of titanium oxides and/or nitrides. The amounts of oxygen and nitrogen in these layers are changing depending on the operating conditions. The laser marking is a modification of the surface contrast properties caused by the chemical, phase and/or surface morphology changes induced when an ablation or a thermal oxidation take place during laser beam interaction with material surface [11, 12]. Some authors suggest that the surface metallic coloration is related to the composition of the color of the bulk oxides [3, 13–15].

During laser marking, many processing parameters may be varied to obtain the desired output, and a huge number of experiments must be performed for that. However, the number of necessary experiments with identified process parameters can be reduced using an experimental design method (DOE). Most studies were performed using Nd:YAG laser to determine the effect of the process parameters on the surface roughness, the surface reflectance, the mark contrast and the depth of removed material. Campanelli et al. [16] used the DOE to investigate the effect of the scanning speed, the frequency, the power, the overlapping degree, and the scanning strategy on the surface roughness and the depth of removed material using factorial analysis. All tests were conducted on aluminum–magnesium alloy specimens using a laser marker machine equipped with a pulsed Nd:YVO4. Leone et al. [17] studied the influence of the multiple laser scanning, the pulse frequency variation, the scanning speed, and the number of scanning repetitions on the material removal rates for different types of wood, using a Q-switched diode-pumped Nd:YAG green laser ($\lambda = 532$ nm). By conducting two experimental approaches: the Taguchi and the response surface methods, it was found out that the engraved depth is strongly affected by the mean power, the pulse frequency, the scanning speed, and the number of passes. By implementing an experimental design approach (Taguchi method and RSM method), Soveja et al. [18] investigated the effect of repetition rate, pulses energy, scanning speed, line-spacing on the mark surface roughness, and material removal rate, on the composite function processed by a Q-switched Nd:YAG laser equipped with a galvanometric head. The factors having a significant influence on the studied objective functions were determined. In addition, mathematical modeling of operating parameters influencing the laser surface texturing process was developed. Results analysis shows that only the frequency and energy of pulses, among studied influencing factors, have a significant influence on laser surface texturing process.

Cicala et al. [19] studied the limitations of metals laser machining and they quantified through a DOE, the influence of the operating parameters on productivity and on the quality of the processed surface for three used materials: aluminum alloy, stainless steel and titanium alloy. The results indicate that the productivity depends mainly on the pulse frequency. The surface roughness was likewise dependent on the pulse frequency and to a lesser extent on the sweeping speed. It was concluded that the surface roughness is minimized by increasing the pulse frequency and by reducing the sweeping speed.

2 The experimental techniques

The laser marking process is performed using heat radiation, to produce high quality marks, by changing the properties and the texture of the substrate surface. Therefore, it is necessary to control the surface roughness Ra and the reflectance R of the treated surface according to the operating parameters.

2.1 The treated material and its preparation

The used material in our study is a commercial pure (CP) titanium substrate (grade 4). Square 10×10 mm^2 samples were prepared, and mechanically polished till 1200 paper grade. To obtain a reference surface with roughness lesser than 0.3 µm. To avoid contamination, the samples were cleaned using ethanol. Circular shape marks of 9 mm diameter were then realized. In Table1, we give the chemical composition of the used substrate (in molar %).

2.2 The laser beam processing parameters

The laser choice is guided by the possibility of obtaining marked patterns depending on the whole material physical properties. In this work, a Q-switched and frequency doubled Nd-YAG green laser (KALUTI) operating at 532 nm and delivering 5 ns pulse duration is used. All experimental tests are obtained using a Gaussian circular laser spots, with a maximum power per pulse of 3 W, a repetition rate of 100 kHz, a maximum energy of 0.3 mJ, resulting in average power of 30 W. The laser beam is focused by a 160 mm focal length lens, giving an average focal spot of about 40 µm on the substrate. The process parameters and the motion of the laser beam over the substrate are controlled by a personal computer and Mark software. The major parameters of the used laser are shown on Table 2.

2.3 The experimental procedure

During marking process, the focused laser beam moves over the metallic surface and creates a thermal reaction within the interaction zone. According to forward and backward motions, passes separated by a fixed line space

Table 1 Chemical composition of the used substrate

CP-Ti substrate					
Substrate composition	Fe	C	O	H	N
(%) Molar	<0.25	<0.08	<0.15	<0.06	<0.0125

Table 2 Used laser marking parameters

Parameters	Description
Laser type	Nd:YAG
Wavelength	532 nm
Pulse duration	5 ns
Operation mode	Pulsed
Scan speed	0–1500 mm/s
Average power	30 W
Pulse frequency	0–100 kHz
Spot laser diameter	10–39 m

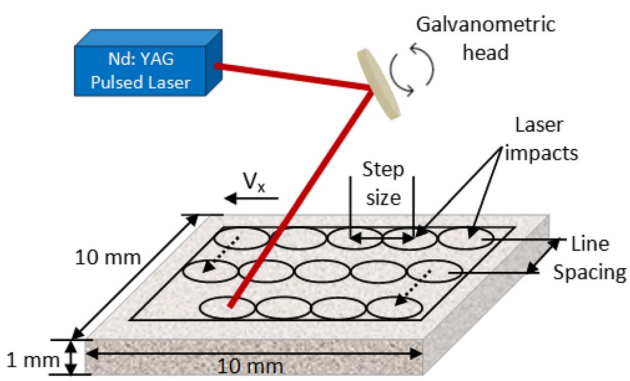

Fig. 1 Schematic representation of laser marking process

are produced, forming series of parallel segments covering a part of the sample surface, as shown on Fig. 1.

The distance between two consecutive laser pulses is related to the scanning speed (Ss) and to the repetition rate (F), which govern the lateral overlap (on x direction) of the irradiated surface, see Fig. 2. The overlapping rate can be calculated by the following equation [16]:

$$\mathrm{OR}_x = \left(1 - \frac{\Delta x}{\phi}\right) \times 100 \quad (1)$$

An increase of the scanning speed or a decrease in the laser pulse frequency makes a low overlapping rate. But it becomes high when frequency is elevated or when the scanning speed is low. Along the y direction, the control of overlapping rate depends strongly on the distance between two passages of laser beam, as given by [20]:

$$\mathrm{OR}_y = \left(1 - \frac{d}{\phi}\right) \times 100 \quad (2)$$

The induced beam light interference effect results in a macroscopic phenomenon that consists in the observation of coloration on the treated surface. The observed coloration depends on the thickness of the induced layer, during laser-substrate surface interaction, which depends strongly on the used operating laser parameters and on the surrounding atmosphere (air).

3 Design of experiment

The design of experiments (DOE) is an organized set of tests prepared in advance, with the objective to determine, with a minimum number of tests and with a maximum of accuracy, the individual and the interactive effects of the various controlled factors on the output results (objective functions). The representation given on Fig. 3 summarizes the studied case and the definition of an experimental plan approach.

The DOE general approach is, therefore, to translate the variation of a response (objective function) on the basis of one or more influence factors by the relation $y = f\left(x_i\right)$ where i vary between 1 and k (where k is the total number of factors).

In our case, the experimental studies were conducted using Taguchi [21] and surface response methods. An analysis of the variance (ANOVA) [22] and a regression model was constituted to find out which parameters have a significant effect on the objective functions and finally to conduct a mathematical model.

3.1 The influencing factors

To analyze the effect of the influence factors on the objective functions that characterizes the quality of the marked surface (minimum surface roughness and maximum surface reflectance), we have conducted an experimental plan (E.P) using a matrix program. The input parameters (influence factors) are selected as they are found to be the most significant marking parameters based on the preliminary tests [3, 23, 24]. The influence factors and their levels of variation are given below in the Table 3.

The used DOE is characterized by 4 factors [Scanning speed (Ss), Repetition rate (F), pumping intensity (I), which is the intensity of diodes pumping, and Line spacing (Ls)], with 4 levels for each factor giving for a full factorial design 256 experimental tests ($x^k = 4^4$, 4 factors with 4 levels). It is obviously noted that dealing with this huge number of tests is a very complex challenge, which requires long time for consuming and costly treatment. A L_{16}Taguchi's Orthogonal Arrays is thus used to conduct the experiment for which details are shown in Table 4, corresponding to the experimental plan. The new design is equivalent to a $4^{(4-2)}$ fractional factorial design, resulting in 16 experimental tests. We give the laser marking results for titanium material, concerning the measured arithmetic roughness Ra (μm), reflectance R (%) and the resulting colors observed on the machined surface

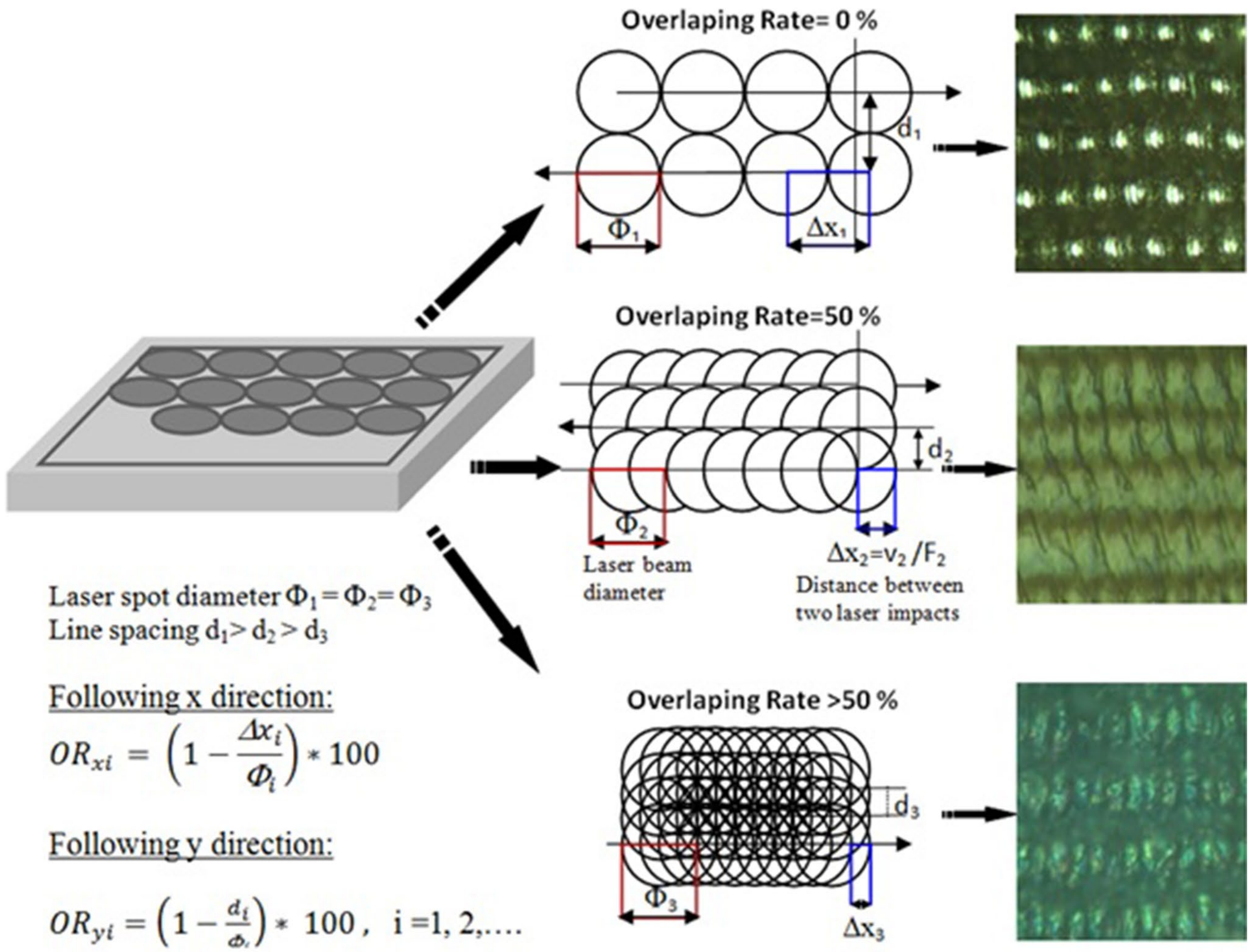

Fig. 2 Horizontal and vertical overlaps produced by laser

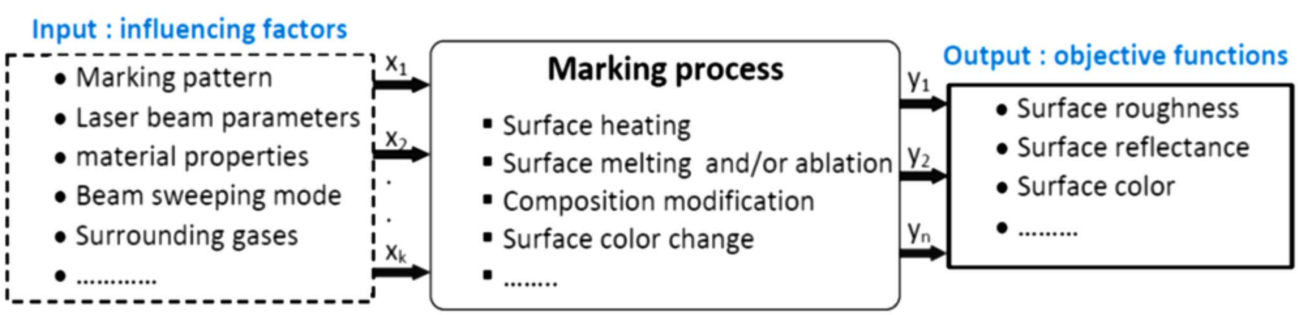

Fig. 3 Simplified diagram of the used experimental plan approach design

corresponding to each test. Optimization of the marking process requires a mathematical model to be established to correlate the desired response and the process control parameters. Response surface methodology (RSM) is employed to design experiments with a reduced number of experimental runs to achieve optimal responses.

3.2 Surface characterization

In the present study, the surface contrast, the reflectance R (%), and the roughness Ra (µm) of the marked pattern are evaluated as output responses of the process. A profilometer Veeko-Vyko NT 9100, assisted by the Vyko-Vision

Table 3 laser marking factors and their levels

Controlled factors	Level 1	Level 2	Level 3	Level 4
Frequency *F* (kHz)	05	10	15	20
Pumping intensity I (A)	24.05	25.90	27.75	29.60
Scanning speed Ss (mm/s)	05	30	100	200
Line spacing Ls (µm)	10	15	20	25

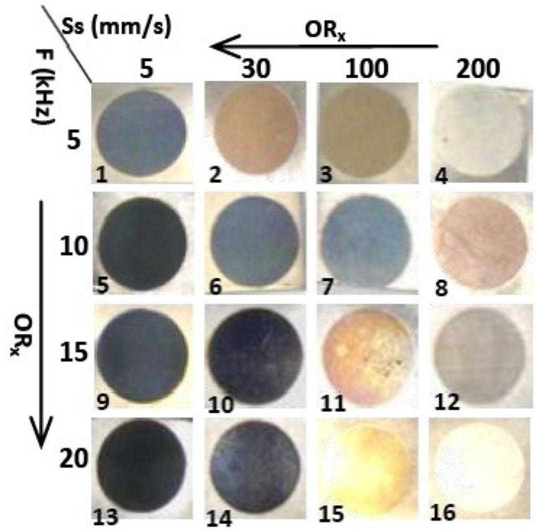

Fig. 4 Coloration induced by laser treatment

software is used to obtain direct values of the roughness Ra in micrometers. The colorimetric measurements (reflectance in %) of the analyzed area for each wavelength in the visible range (400–700 nm) were carried out with a Konica-Minolta CM 3500d universal colorimeter. The morphology of the laser scanned samples was examined by means of a JEOL, JSM-6360LVscanning electron microscope (SEM).

4 Results and discussion

4.1 Resulting colors

Example of different colors obtained on titanium sample by varying the processing parameters under normal atmospheric conditions is shown on Fig. 4. It is noticed that the colors vary from the uncolored to the dark blue, and from the obtained palette, it can be observed that the scanning speed plays an important role on the marked surface quality. Indeed, the marking contrast decreases rapidly when the scanning speed increases. For the lower speed (5 mm/s), the treated surface contrast is far dark as it is clearly observed for the tests 1, 5, 9 and 13. Another important parameter affecting the contrast is the overlapping rate (OR_x), corresponding to the number of superimposed pulses on the same area, resulting from the combination of the scanning speed and the repetition rate (frequency), as mentioned in Table 4.

Table 4 Taguchi design matrix and measured values

Test No.	Process control parameters				Measured values of objective functions			Combination of process parameters
	F (kHz)	Ss (mm/s)	I (A)	Ls (µm)	Ra (µm)	R (%)	Colors	OR_x(%)
1	1	1	1	1	1.628	11.57	Blue	97.43
2	1	2	2	2	0.223	34.17	Golden	84.61
3	1	3	3	3	0.243	19.21	light Golden	48.71
4	1	4	4	4	0.188	21.04	light Grey	00.00
5	2	1	3	2	1.998	06.05	Grey/dark Blue	98.71
6	2	2	4	1	1.032	21.69	dark Green	92.30
7	2	3	1	4	1.827	34.06	Blue	74.35
8	2	4	2	3	0.294	26.85	Yellow	48.71
9	3	1	4	3	0.820	06.00	dark Grey	99.14
10	3	2	3	4	0.458	05.71	Purple	94.87
11	3	3	2	1	0.236	09.10	Golden	82.90
12	3	4	1	2	0.208	06.71	light Grey	65.81
13	4	1	2	4	4,960	11.73	dark Grey	99.35
14	4	2	1	3	0.365	09.64	Purple	96.15
15	4	3	4	2	0.200	32.93	light Golden	87.17
16	4	4	3	1	0.122	53.43	Uncolored	74.35

4.2 Effect of the processing parameters on Ra and R

To investigate the processing parameters effects on the average surface roughness Ra based on the Taguchi design, the graph of each plotted parameter corresponding to different test conditions are illustrated in Fig. 5. From the results, one can conclude that the scanning speed has the main influence on the surface quality. It is noted indeed that the surface roughness decreases when the scanning speed increases, and that the lower surface roughness value is obtained for the processing parameters $F_1Ss_4I_1Ls_1$, where the indices correspond to the level of the processing parameter. This phenomenon can be explained by the fact that when a metallic surface is irradiated by a laser beam, it causes surface temperature increasing due to focusing an amount of laser energy into a small region, and the variation of the surface morphology during laser scanning at given speed is related to the laser energy density. For a given pulse frequency, when the laser beam is moved over the material surface at low scanning speed, the laser exposure time and the number of superimposed impacts (overlapping rate) becomes higher, producing a high laser energy density, and consequently a surface temperature increase. If the surface temperature reaches the melting temperature, the viscous flow causes smoothening of the surface. On the other hand, if the surface temperature exceeds the melting temperature, vaporization occurs, resulting in crater structures formation and beads after solidification of the melt.

We have concluded that for the set of operating parameters F_1 Ss_4 I_1 Ls_1, a lower surface roughness is obtained, knowing that scanning speed is the more influenced parameter with its higher value (200 mm/s), followed by the pumping intensity, where its corresponding value in the level 1 is the most lower (24.05 A). It is found in literature [25, 26] that the surface roughness is inversely proportional to the laser scanning speed. The analysis of the diagram represented in Fig. 5 shows that for a better surface roughness, the more appropriate scanning speed is 200 mm/s. For a 95% confidence level, only scanning speed has a significant influence on the surface roughness Ra.

On Fig. 6, we can observe the main effects of surface reflectance R plot, which is used to predict the optimum levels of the process parameters for maximum R. According this figure, the predicted optimal surface reflectance R value is obtained for F_1 Ss_4 I_1 Ls_3 as reported in Table 4. It can be concluded that, the scanning speed with its different variation levels is the process parameter which has the main effects on both

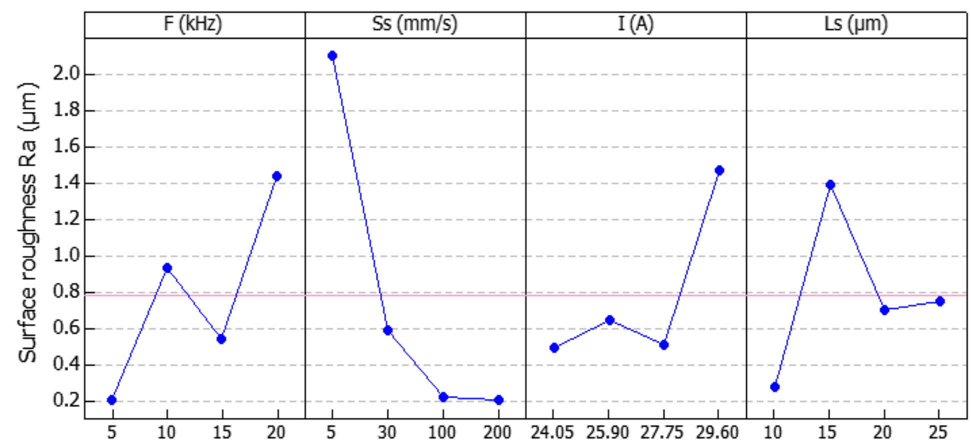

Fig. 5 Main effect plot for surface roughness Ra

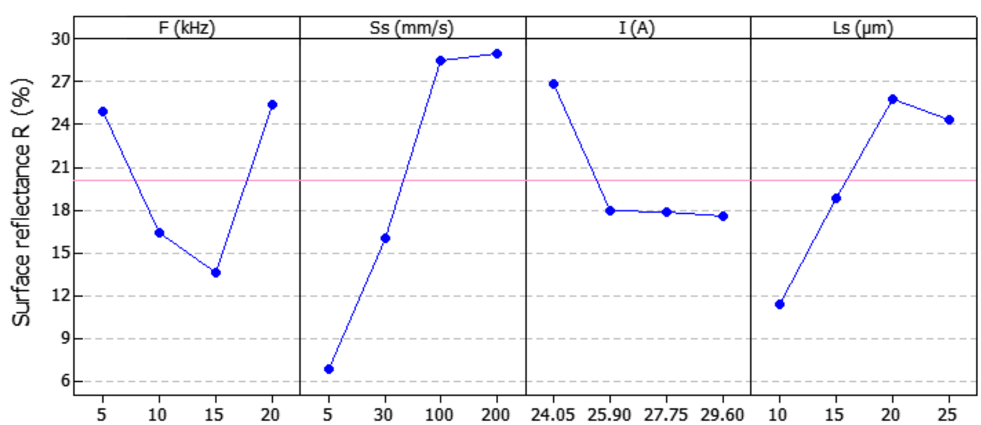

Fig. 6 Main effect plot for surface reflectance R

surface reflectance and surface roughness. The most influential factors on the reflectance are scanning speed, followed by pumping intensity, line spacing and then pulse frequency. For a 95% confidence level, scanning speed and pumping intensity have a significant influence on the surface reflectance.

4.3 Analysis response surface designs: results for Ra and R

According to the diagram of influencing factors generated effects (Figs. 5, 6), we select two factors (scanning speed and pumping intensity) due to their high influence on the examined objective functions. A central composite second order design is considered as one type of response surface design, to optimize the surface marking process. The experimental matrix is composed of $2k$ factorial design points and consists in performing experiments at $2k$ axial design points of the square at ± 1 levels, for axial points at ± 1.414 levels and center point at 0 levels [27]. In our case $k = 2$ is the number of significant influencing factors.

The variation levels of influencing factors are presented on Table 5, where the chosen central point for the scanning speed is 102.5 mm/s and that of for the pumping intensity is 26.82 A. To simplify the calculations, experimental design with equivalence for coded values of the thirteen (13) experiments is planned. The fitted values of the experimental measurements are given in Table 6.

The ANOVA results given on Table 7 show the statistical significance of each operating parameter based on the percentage of contribution and the *p* values. It is clear from the results that the scanning speed x_1, and its quadratic term x_1^2 significantly affect Ra and R. The *p* values are lower than 0.05 for the two objective functions, which indicate that the estimated regression model is significant at 0.05 levels. It is also remarkable that the interactive term effect between scanning speed and pumping intensity ($x_1 \times x_2$) have the lowest significant effects on the objective functions Ra and R. The highest percentage contribution for Ra and R is observed at scanning speed x_1 of 53.38 and 65.55%, respectively. The column percentage contribution given in the ANOVA table indicates the appropriate measure of the relative importance of each term in the model to the total sum of square [28].

Table 6 Central composite design matrix in coded units and predicted objective functions

Test No.	Influence factors		Objective functions	
	x_1	x_2	Ra (μm)	R (%)
1	−1	−1	1.557	12.77
2	1	−1	0.510	34.80
3	−1	1	1.592	19.24
4	1	1	0.463	20.49
5	−1.414	0	3.421	05.31
6	1.414	0	1.882	21.76
7	0	−1.414	−0.585	32.89
8	0	1.414	−0.593	27.34
9	0	0	0.687	07.85
10	0	0	0.687	07.85
11	0	0	0.687	07.85
12	0	0	0.687	07.85
13	0	0	0.687	07.85

4.4 Development of a mathematical model using regression analysis

A statistical ANOVA is employed to determine the significance of a mathematical model taken from regression analysis. The relationship between the input consisting of the marking conditions [scanning speed (Ss) and punping intensity (I)] and the resulting effects of the output, designated by Y [surface roughness (Ra) and surface reflectance (R)] is presented as :

$$Y = f\left(x_i, x_j\right) \tag{3}$$

where f is the response function. The two second order regression models (polynomial) are constituted to estimate the surface roughness and the surface reflectance as a function of scanning speed x_1 and as a function of pumping intensity x_2 is the nonlinear quadratic model given in Eq. (4):

$$Y = \beta_0 + \sum_{i=1}^{m} \beta_i x_i + \sum_{i=1}^{m} \beta_{ii} x_i^2 + \sum_{\substack{i=1 \\ i \neq j}}^{m} \sum_{j=1}^{m} \beta_{ij} x_i x_j \tag{4}$$

where Y is the corresponding objective function, x the coded values of the influencing factors, m the number of factors and β_0, β_i, β_{ii}, β_{ij} are the regression coefficients given in

Table 5 The most influencing factors and their levels

Influence factors	Codes	Levels				
		−1.414	−1	0	+1	+1.414
Ss (mm/s)	x_1	5.00	33.55	102.50	171.44	200.00
I (A)	x_2	24.05	24.86	26.82	28.78	29.60

Table 7 Anova table for Ra (µm) and R (%) based on general linear model

Objective functions	Terms	DF	SS	MS	*F*	*P*	Percentage of contribution
Ra (µm)	x_1	1	1.390	1.390	52.59	0.000	53.38
	x_2	1	4.10^{-4}	1.381	52.28	0.000	0.015
	${x_1}^2$	1	1.024	1.339	50.67	0.000	39.32
	${x_2}^2$	1	0.003	0.031	01.19	0.311	0.115
	$x_1 \times x_2$	1	6.10^{-5}	6.10^{-5}	00.00	0.964	0.002
	Error	7	0.185	0.026	-	-	7.104
	Total	12	2.604	-	-	-	100
S = 0.162594 R-Sq = 92.89% R-Sq (adj) = 87.82%							
R (%)	x_1	1	862.77	862.77	199.76	0.000	65.55
	x_2	1	13.70	56.27	13.03	0.009	01.04
	${x_1}^2$	1	30.78	825.23	191.07	0.000	02.34
	${x_2}^2$	1	270.90	97.13	22.49	0.002	20.58
	$x_1 \times x_2$	1	107.90	107.90	24.98	0.002	08.20
	Error	7	30.23	4.32	–	–	02.30
	Total	12	1316.28	–	–	–	100.00
S = 2.07824 R-Sq = 97.70% R-Sq(adj) = 96.06%							

Table 8. The reduced quadratic mathematical model used to predict the surface roughness and surface reflectance in terms of coded factors are expressed respectively in the Eqs. (5) and (6) as follows:

$$\mathrm{Ra}(\mu\mathrm{m}) = 0.687 - 0.544x_1 - 0.003x_2 + 0.981x_1^2 - 0.638x_2^2 - 0.020x_1x_2 \quad (5)$$

$$\mathrm{R}(\%) = 7.850 + 5.819x_1 - 1.961x_2 + 2.844x_1^2 + 11.137x_2^2 - 5.194x_1x_2 \quad (6)$$

Table 9 summarises the ANOVA of each response and shows the significant quadratic model terms for the both objective functions: surface roughness and surface reflectance. According to the model, the *F*-values 18.30 and 59.55 corresponding to surface roughness and surface reflectance, respectively, are too much high, and indicates that they are of high significance. From this table, the lack-of-fit *p*-value is important (greater than 0.05) and may be insignificant. The *F*-value of 18.30 indicates that the model is significant. In the case of the surface roughness, the scanning speed (x_1), the pumping intensity (x_2), their interactive term ($x_1 \times x_2$) and their second order term, are all significant model terms. It can be concluded that the predicted mathematical model built above agree very well with the experimental data. The Figs. 7 and 8 show the plot of the calculated objective functions surface roughness and surface reflectance using Eqs. (5) and (6) as function of the measured data. One can conclude that the predicted models for both surface roughness and surface reflectance are in well adequacy with the measured results, and statistically acceptable for a confidence level of 95%. The correlation coefficients (R^2) [28] can be calculated using relation (8). Their values are 93% for Ra and 98% for R.

$$\mathrm{R}^2 = \frac{SS_{\mathrm{Total}} - SS_{\mathrm{Error}}}{SS_{\mathrm{Total}}} \quad (8)$$

The developed mathematical model can be used to generate contour plots, to show the effect of process factors on the objective functions. On the Figs. 9 and 10, we represent the dependence of surface roughness and surface reflectance, as functions of the scanning speed and the pumping intensity. The analysis shows that, the scanning speed is the most influential factor on surface roughness and surface reflectance. We can thus draw on the contour plots of Fig. 9, are presentation of the interaction between pumping intensity and laser beam scanning speed on the roughness and reflectance of the processed surfaces by laser. By increasing the scanning speed Ss (mm/s), the surface

Table 8 Estimated regression coefficients for Ra (µm) and R (%)

Coef	Regression coefficients					
	β_0	β_1	β_2	β_{11}	β_{22}	β_{12}
Ra (µm)	0.687	−0.544	−0.003	0.981	−0.638	−0.020
R (%)	7.850	5.819	−1.961	2.844	11.137	−5.194

Table 9 Anova table for polynomial regression of order 2 for Ra (µm) and R (%)

Objective functions	Degree of freedom *DF*	Sum of square SS	Mean square MS	*F*	*P*
Ra (µm)					
Regression	5	2.419	0.483	18.30	0.001
Linear	2	0.004	0.002	00.08	0.925
Square	2	2.414	1.207	45.67	0.000
Interaction	1	6.10^{-5}	6.10^{-5}	0.000	0.964
Residual error	7	0.185	0.026	–	–
Lack-of-fit	3	0.003	0.001	0.002	0.994
Pure error	4	0.181	0.045	–	–
Total	12	2.604	–	–	–
R (%)					
Regression	5	1286.05	257.210	59.55	0.000
Linear	2	301.68	150.840	34.92	0.000
Square	2	876.47	438.236	101.46	0.000
Interaction	1	107.90	107.900	24.98	0.002
Residual error	7	30.23	4.319	–	–
Lack-of-fit	3	4.32	1.438	0.22	0.877
Pure error	4	25.92	6.480	–	–
Total	12	1316.28	–	–	–

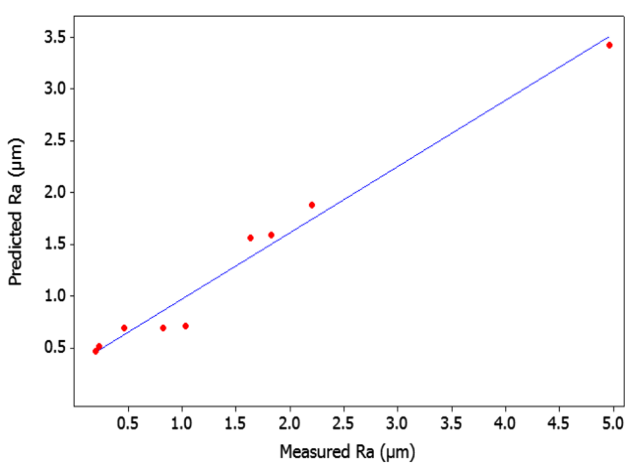

Fig. 7 Predicted vs. measured surface roughness Ra

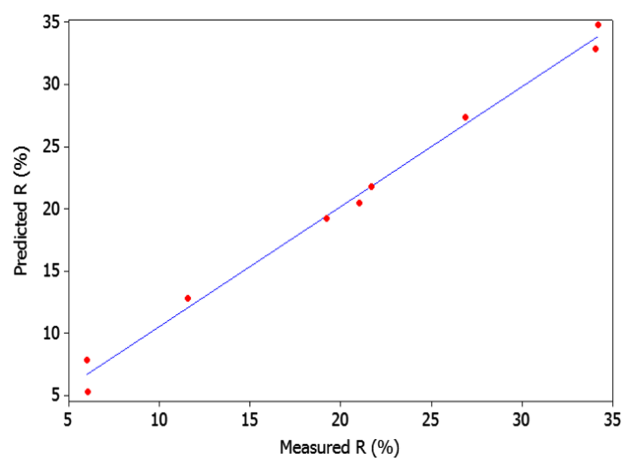

Fig. 8 Predicted vs. measured surface reflectance R

reflectance R gain increase sat low pumping intensities *I*(*A*). As it is known, maximum reflectance is desired to provide good quality of mark, therefore, according to this plot; an optimum (maximum) reflectance is achieved with the scanning speed interval between 100 and 200 mm/s.

Meanwhile, this observation is not evident from the contour plot of surface roughness. On the combined effects of the pumping intensity and the scanning speed on the surface roughness plotted in Fig. 10, we can note that roughness variation increases linearly with the decrease of the scanning speed and independently of the pumping intensity. As it can be seen from the presented contours, the surface roughness decreases when the surface is processed at high scanning speed. The optimal domain for minimizing the surface roughness is situated in area corresponding to 150–180 mm/s and represents the optimal domain for maximizing the surface reflectance. Therefore, based on the given process parameters, scanning speed and pumping intensity, we can conclude that if a high reflectance of the treated surface is required, then it is recommended that the scanning speed values to be greater than 100 mm/s.

This result can be confirmed by the analysis of the surface morphology of samples produced with degree of overlap of 97, 84, 48 and 0% as shown in Fig. 11,

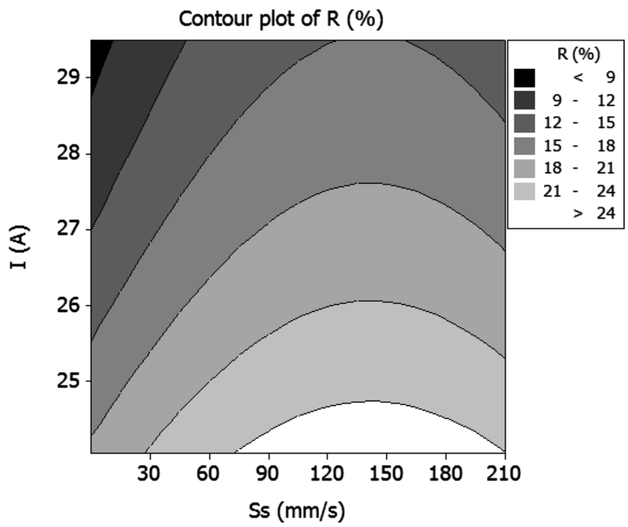

Fig. 9 Contour surface plot of R (%) vs. scanning speed and pumping intensity

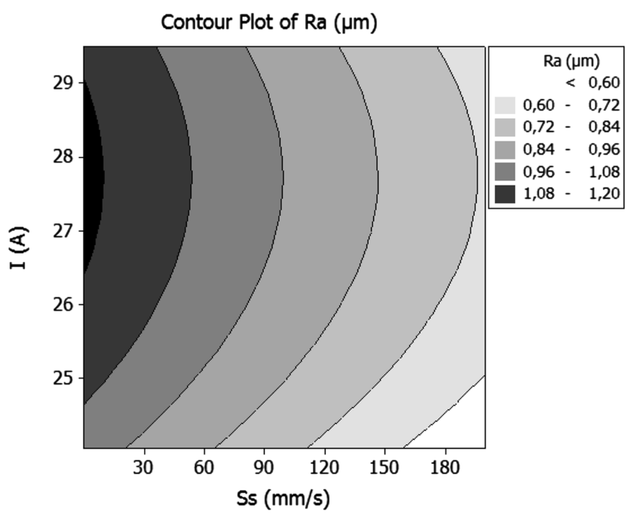

Fig. 10 Contour surface plot of Ra (µm) vs. scanning speed and pumping intensity

corresponding, respectively, to the tests 1, 2, 3 and 4. The pictures obtained by scanning electron microscopy (SEM) show the surface appearance and the quality of the processed samples. From the obtained images, we can conclude that the most influent processing parameter is still the scanning speed.

The effect of the overlapping rate deduced from combination of the employed processing parameters on surface roughness is shown on these pictures. Surface roughness change inversely to the scanning speed and linearly with the overlapping rate of the laser impacts. The degree of overlap of 97% produces the highest surface roughness (Ra = 1.628 µm) for the first treated serie1 to 4 due to the solidified molten material ejected behind the laser shots.

4.5 Effect of the parameters combination on Ra and R

The effect of the overlapping rates on surface roughness and reflectance is reported in Fig. 12. The results indicate that the combined effects of the frequency and the scanning speed have an influence on the overlapping rate as given by Eq. (1). The increase in the pulses frequency results in an increase of the overlapping rate, which causes an increase in the energy per unit area, and consequently leads to a higher roughness and lower reflectance. For all tests, the higher values of Ra (µm) and the lower values of R (%) are obtained at higher overlapping rates.

4.6 Effect of the scanning speed on Ra and R

The reported results on Fig. 13 show the evolution of surface roughness and the surface reflectance as a function of the scanning speed. We note that the minimum Ra values are obtained for all frequencies when the scanning speed becomes higher and greater than 100 mm/s. In previous works [18, 29], it was indicated that a rapid processing is required to obtain a better marked surface, which is in accordance with our results. It is clearly shown for the surface reflectance evolution vs. the scanning speed that the maximum reflectance values are obtained at higher scanning speeds. On the figure, we can see how the surface roughness Ra affects negatively the reflectance of incident white light. For very smooth surfaces which have mirror appearance (low Ra), the incident white light is totally reflected. Inversely, for a higher rough surfaces (high Ra), the white light is not reflected but diffused in all directions; therefore, the surface has a matt appearance (see Table 5).

5 Conclusion

We have conducted a statistical analysis and an optimization of the pulsed Nd:YAG nanosecond laser marking process of titanium substrate. A hybrid experimental design approach, Taguchi and response surface methods for the responses optimization were used to analyze the conditions for coloring of titanium (CP) surfaces and to investigate the effects of process parameters (influence factors) on the roughness and reflectance of the treated surface.

From the obtained results, the main conclusions are as follows:

- For the control of the marked surface quality to optimize the process of colors contrast producing, the effect

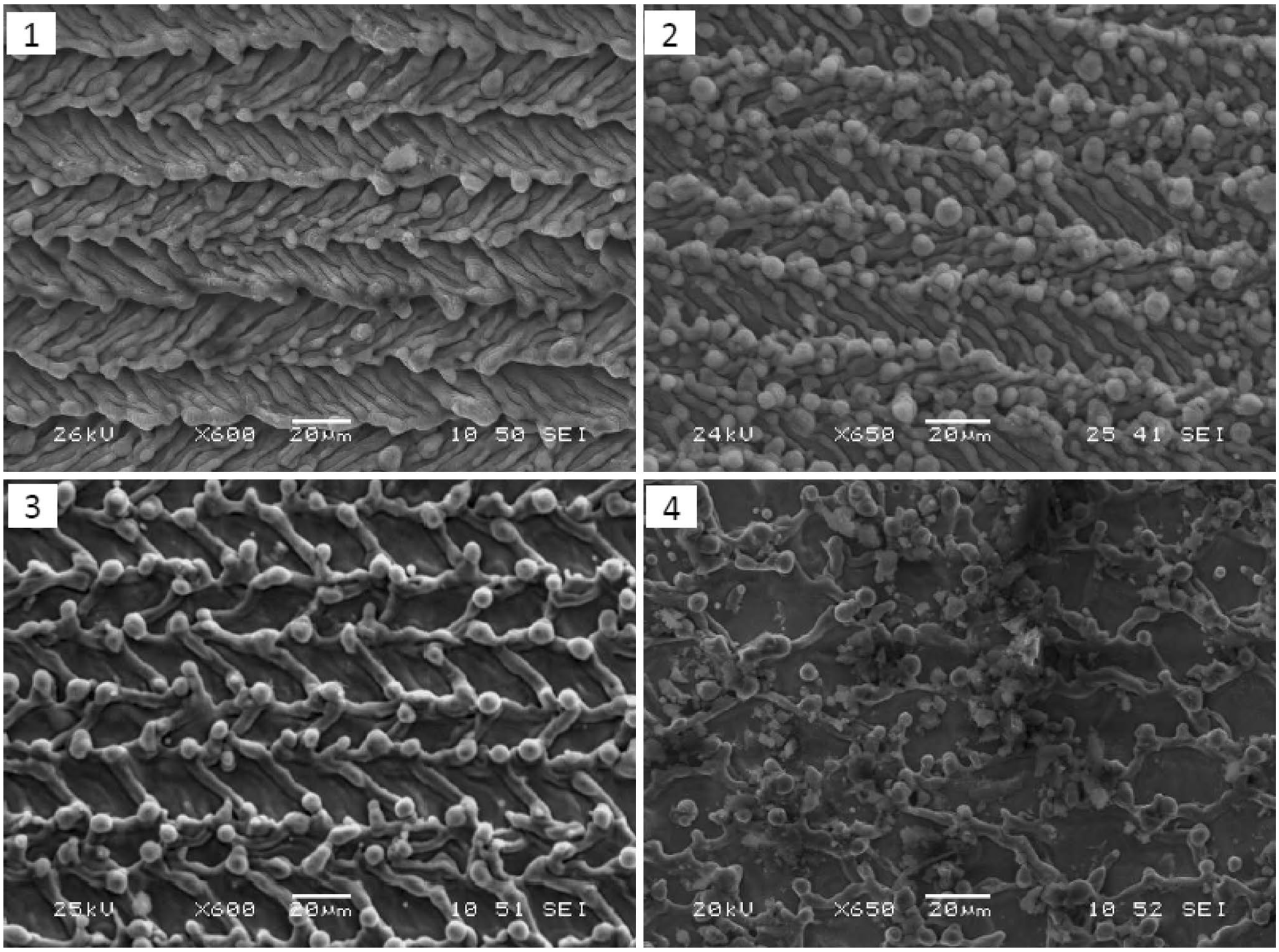

Fig. 11 SEM surface morphology of samples 1, 2, 3 and 4

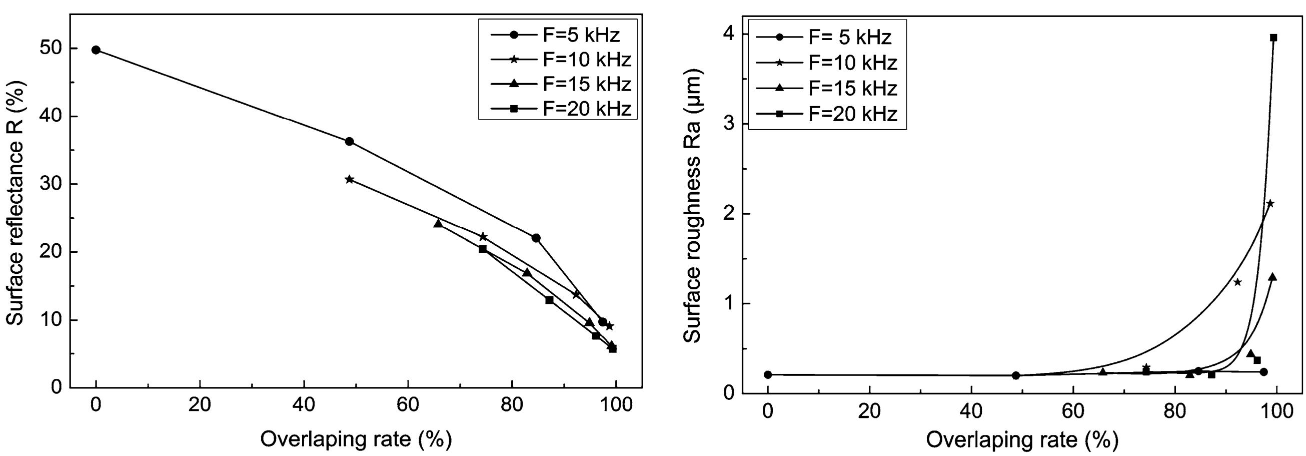

Fig. 12 Effect of the overlapping rate on Ra (µm) and R (%)

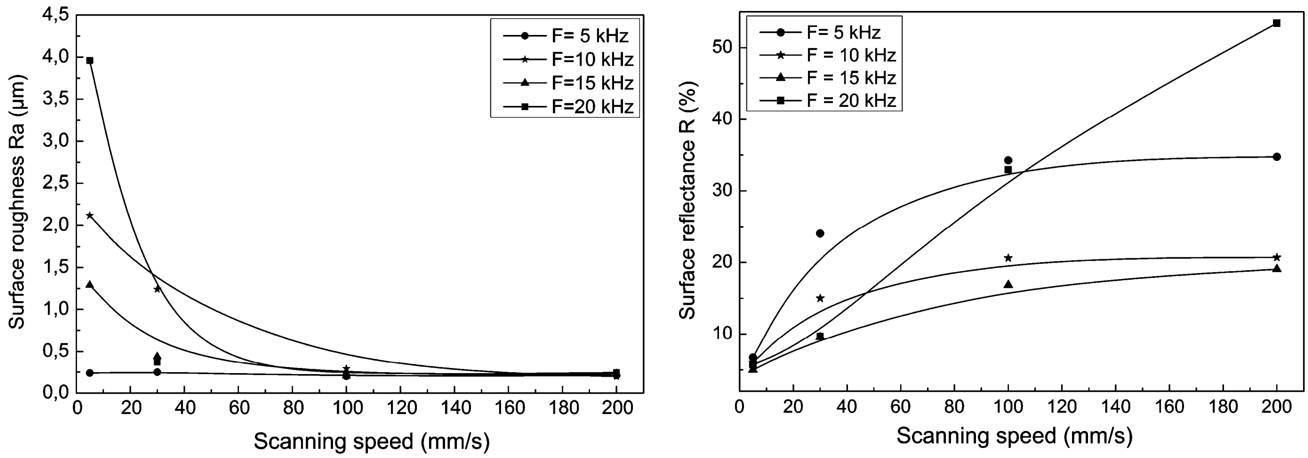

Fig. 13 Effect of the laser beam scanning speed on Ra (µm) and R (%)

of the laser parameters (influence factors) was investigated.

- Various controlled colors have been obtained by varying the laser beam parameters (Fig. 4).
- The factors having a significant influence on studied objective functions are the scanning speed and the pumping intensity (Figs. 5, 6).
- The appropriate process conditions for a lower Ra and higher R is achieved using a scanning speed of 200 mm/s, a line spacing of 20 mm, a pumping intensity of 24.05 A and a frequency of 5 kHz, as observed on (Figs. 5, 6).
- High reflectance and good roughness can be obtained by choosing the right process conditions: High scanning speed and low pumping intensity.
- The overlapping rate (OR_x) affects significantly the mark contrast, the surface roughness and the surface reflectance. The highest values for Ra were observed for higher OR_x (test 13 in Table 4).
- The Central composite design (CCD) was applied to predict both surface roughness and surface reflectance.
- The regression analysis based on the mathematical model prediction of R and Ra are implemented and compared with the experimental values (Fig. 7). The results showed that the effect of laser beam scanning speed is statistically significant at 0.05 levels.
- The analysis of Contour Surface Plot of both surface roughness and surface reflectance vs. scanning speed and pumping intensity (Figs. 9, 10) allows determining the optimal operating conditions for improving surface quality. The white area in the graph gives values of process parameters, minimizing Ra (µm) and maximizing R (%).
- The optimal set of influencing factors, which enable the minimization of surface roughness (<0.55 µm), and maximization of surface reflectance are a 24.05 A of pumping intensity and scanning speed in the range of 100–200 mm/s.

References

1. John C. Ion: Laser processing of engineering materials: principles, procedure and industrial application (Elsevier, 1st edn, 2005)
2. C. Velotti, A. Astarita, C. Leonea, S. Genna, F. Memola Capece Minutolo, A. Squillace: Procedia CIRP. **41**, 975 (2016)
3. A. Peréz del Pino, P. Serra, J.L. Morenza. Appl. Surf. Sci. **197–198**, 887 (2002)
4. A.J. Antonczak, L. Skowronski, M. Trzcinski, V.V. Kinzhybalo, L.K. Lazareka, M. Krzysztof, Abramski. Appl. Surf. Sci **325**, 217 (2015)
5. S. O'Hana, A.J. Pinkerton, K. Shoba, A.W. Gale, L. Li, Surf. Eng. **24**, 147 (2008)
6. T.W. Ng, S.C. Yeo, J. Mater. Process. Technol. **104**, 280 (2000)
7. L. Lavisse, P. Berger, M. Cirisan, J.M. Jouvard, S. Bourgeois, M.C. Marco de Lucas, J. Phys. D Appl. Phys. **42**, 8 (2009)
8. F.J.C. Braga, R.F.C. Marques, E.A. Filho, A.C. Guastaldi, Appl. Surf. Sci. **253**, 9203 (2007)
9. A. Peréz del Pino, J.M. Fernandez-Pradas, P. Serra, J.L. Morenza, Surf. Coating Technol. **187**, 106 (2004)
10. Z. Hongyu, Q. Hong, L.G. Cher, W. Xincai, C. Qiong, E.P. Alvarez, Singapore patent application No. 200200661-7 Feb (2002)
11. C. Langlade, A.B. Vannes, P. Piccinini, G. Baldi, in *Surface modification technologies. XI. The institute of materials*, ed. by T.S. Sudarshan, M. Jeandin, K.A Kho (London, 1998), p 634
12. C. Langlade, A.B. Vannes, J.M. Krafft, J.R. Martin, Surf. Coating Technol. **100–101**, 383 (1998)
13. L. Lavisse, D. Grevey, C. Langlade, B. Vannes, Appl. Surf. Sci. **186**, 150 (2002)
14. E. Clauss, Neiss: Mise en forme de faisceaux de lasers de puissance dans le proche infrarouge par éléments diffractifs. Thèse de doctorat, Université Louis Pasteur de Strasbourg, France (2007)
15. M.S. Brown, C.B Arnold, Springer series in materials. Science **135**, 91 (2010)

16. S.L. Campanelli, G. Casalino, N. Contuzzi, Optics Laser Technol. **52**, 48 (2013)
17. C. Leone, V. Lopresto, I. De Iorio, Opt. Lasers Eng. **47**, 161 (2009)
18. A. Soveja, E. Cicala, D. Grevey, J.M. Jouvard, Optics Laser Eng. **46**, 671 (2008)
19. E. Cicala, A. Soveja, P. Sallamand, D. Grevey, J.M Jouvard, J. Mater. Process. Technol. **196**, 393 (2008)
20. W. Pacquentin, Contribution à l'étude des propriétés physico-chimiques des surfaces modifiées par traitement laser. Thèse de doctorat, Université de Bourgogne, France (2011)
21. M.G. Vigier, Pratique des plans d'expériences-méthodologie Taguchi (Les Editions d'Organisation 1988)
22. MINITAB User guide: version 17.3.0, USA, (2014–2016). http://www.minitab.com
23. L. Lavisse, J.M. Jouvard, L. Imhoff, O. Heintz, J. Korntheuer, C. Langlade, S. Bourgeois, M.C. Marco de Lucas, Appl. Surf. Sci. **253**, 8226 (2007)
24. S. Genna, C. Leone, V. Lopresto, L. Santo, F. Trovalusci, Int. J. Mater. Form. **3**, 1115 (2010)
25. S. Kasman, I.E. Saklakoğlu, Adv. Mater. Res. **264–265**, 1258 (2011)
26. F. Agalianos, S. Patelis, P. Kyratsis, E. Maravelakis, E. Vasarmidis, A. Antoniadis, World Acad. Sci. Eng. Technol. **59**, 1242 (2011)
27. A.N. Chatterjee, S. Kumar, P. Saha, P.K. Mishra, A.R. Choudhury, J. Mater. Process. Technol. **136**, 151 (2003)
28. P.K. Krishnaiah, Shahabudeen: Applied design of experiments and Taguchi methods (Estern economy edition, New Delhi 2012)
29. D.P. Hiscocks, Syscomp Electronic Design Limited. September 16 (2011)